**RESEARCH ARTICLE**

# Optimal Control of Non-Holonomic Robotic Systems Based on Type-3 Fuzzy Model

**LILI WU[1], HAIYAN HUANG[1], MENG WANG[2], KHALID A. ALATTAS[3], (Member, IEEE), ARDASHIR MOHAMMADZADEH[4], AND EBRAHIM GHADERPOUR[5]**

[1]School of Intelligent Manufacturing, Zhejiang Guangsha Vocational and Technical University of Construction, Dongyang 322100, China
[2]Jiangsu Huibo Robot Technology Company Ltd., Suzhou 215000, China
[3]Department of Computer Science and Artificial Intelligence, College of Computer Science and Engineering, University of Jeddah, Jeddah 23890, Saudi Arabia
[4]Multidisciplinary Center for Infrastructure Engineering, Shenyang University of Technology, Shenyang 110870, China
[5]Department of Earth Sciences, Sapienza University of Rome, 00185 Rome, Italy

Corresponding author: Ebrahim Ghaderpour (ebrahim.ghaderpour@uniroma1.it)

**ABSTRACT** The paper studies the control of wheeled land mobile robots (MRs) using nonlinear equations and non-holonomic dynamic constraints. Due to the complex and unpredictable nature of the environments in which these robots operate, designing a controller for them is a challenging task. Uncertainties in the system further compound the problem. To tackle these challenges, this paper proposes a novel approach based on type-3 (T3) fuzzy logic systems (FLSs) for system identification and parameter estimation. The T3-FLSs are used to create an online model of the MRs dynamics, which is then used to design a model-based control system. To account for the approximation error of T3-FLSs and the effect of un-modeled dynamics and constraints, an optimal supervisor is designed. The supervisor compensates for any error in the model and ensures that the control system remains stable under symmetrical constraints. A Lyapunov analysis is conducted to verify the stability of the system. The simulations demonstrate that the proposed controller yields excellent results even in the presence of non-holonomic constraints and fully unknown dynamics. The findings of this study offer significant insights into the challenges associated with controlling MRs and provide a promising solution to address these issues.

**INDEX TERMS** Adaptive control, fuzzy control, non-holonomic, optimal control, robotic systems, symmetrical constraints, type-3 fuzzy logic.

## I. INTRODUCTION

Mobile robots (MRs) are the most useful and popular robots due to their efficiency and simple structure. As a result, research on this category of robots has received a lot of attention. This type of robot is a good replacement for humans in dangerous places. Today, with the expansion of control knowledge, wheeled land mobile robots are being considered. The format of working in different spaces, the lack of working space limitations, scientific adaptability, mechanical simplicity, etc., are among the important capabilities of this category of robots. These robots have three degrees of freedom in the plane, including spatial coordinates and orientation. Meanwhile, non-holonomic robots control the

The associate editor coordinating the review of this manuscript and approving it for publication was Haibin Sun.

spatial coordinates and orientation of the robot by adjusting the torque of two motors on the wheels. The main problem of these robots is the non-linearity of the governing kinematic equations, due to which the non-linear controllers play an important role in regulating the robots' behavior [1], [2].

The nonlinearity of the equations along with the non-holonomic dynamic constraints and the multi-input-multiple-output nature of these systems have complicated the design of the controller for these robots. Also, due to the operation of these robots in complex environments and the presence of factors such as friction and uncertainties in the system, the controller design process is usually associated with trial and error. The main disadvantage of the trial and error method is not finding optimal control parameters and the dependence of the designed controller on the selected platform. One of the proposed approaches to find

a solution for the above-mentioned problems is to use system identification methods to find the system model and estimate its parameters [3].

Common mobile robots, such as robots with quasi-machine structures or differential thrust, face limitations in movement. The quasi-machine moving robot cannot move sideways and rotate in place. A differential moving robot can rotate in place, but it is still not possible to move sideways for this robot either. In omnidirectional moving robots, there are movement limitations. The above limitations do not exist and the robot has the possibility to move in any direction. Non-holonomic omnidirectional robots have a limitation in tracking a path whose curvature curve is not continuous, and they have to stop and adjust the direction of the wheels before continuing the path. In fact, it is possible before giving the velocity vector for a non-holonomic omnidirectional robot, it is necessary for the robot to come to a complete stop to adjust the position of the wheels according to the new velocity vector.

Holonomic omnidirectional robots can follow any velocity vector without any initial adjustment, regardless of their state. Holonomic robots are classified into two classes. The first category is robots whose wheels have a special mechanism. However, the second category of holonomic robots uses simple non-holonomic wheels. Universal wheels are equipped with rollers on the wheel circumference that allow passive free rotation around tangential rotational axes. In this case, the wheel will not show resistance against the movements perpendicular to the wheel surface. The use of a sphere, whose axis of rotation can be changed at any moment, forms the basic idea of another group of holonomic wheels, a number of rollers that rotate the sphere in one direction and in another direction. They have no resistance against its movement, they are installed on a spherical wheel to provide its thrust [4].

In last decades, extensive research has been carried out in the field of control systems of dynamic robots and many articles have been published in this direction. It can be said that the main part of this investigation is the problem of rejecting the path by the robot in the presence of uncertainty. There are many difficulties in implementing model-based controllers. One of the most important of these problems is the inability to accurately model. In addition, the presented models will be too complex to make the design difficult for the controller. Inaccuracy in modeling, uncertainty in model parameters, and unmodeled dynamics are other challenging issues in control model-based robots [5].

### A. REVIEW

As mentioned, MR is a non-linear system with limited move-ment, which, with its simple structure and high efficiency, is used in medicine as a smart wheelchair, in rescue for detection and rescue, in military industries for mine detection and in industry. It has many uses as a warehouse and cargo carrying robot. In this sense, the control of the MR is very important. In the structure of this robot, the wheels play an important role. To move these wheeled robots, they use a small number of connections between the robot body and the wheels; Therefore, the connection of the wheels to the body, correspondingly, the connection of the actuators to the wheels and factors such as the way of connection, the type of wheels, disturbances, dynamic and static frictions in each wheel and connection, access to the dynamic equations of the robot, or in other words, precise modeling of the robot It causes problems for the mobile. On the other hand, in case of access to these factors, modeling is difficult, even in the case of correct modeling, the design of the controller will be very complicated and this will increase the construction costs. The presented solutions can be divided into two parts:

- Control of MRs based on kinematics.
- Control of MRs based on kinematics and dynamics.

In the control of the MRs based on the kinematics, the traditional closed-loop stable kinematic control technique is used [6]. In this method, the controller is constructed based on the kinematic equations without considering the dynamic equations of the robot; Therefore, this control method cannot ensure the stability in the presence of structural and non-structural uncertainties. For this reason, to overcome these problems, the researchers presented the control methods using both kinematics and dynamics. In this approach, researchers use techniques such as feedback linearization [7], neural-fuzzy control [3], [8], adaptive control [9], adaptive neural-fuzzy control [10], [11], and FLS-based optimal control [12], [13].

Over the past few decades, researchers have focused more on studying the kinematic control of MRs while relatively less attention has been given to their dynamic control. However, in engineering, dynamic control is more practical and beneficial as they involve torque input. As a result, it is advisable to prioritize the study of dynamic control in wheeled mobile robots. In the field of dynamic controlling of these systems using the base model control method, many valuable works have been done. In [14], the adaptive control method has been used to control a mobile robot with a non-holonomic constraint that has unknown dynamic parameters. In [15], an adaptive controller is proposed for tracking the time reference path by a wheeled mobile robot. In [10], an adaptive neural SMC has been designed to follow the reference path by a wheeled mobile robot. In [16], by combining the SMC control method and the inverse dynamic method, tracking of the time reference path has been done by a wheeled mobile robot that has uncertainty in the model and external disturbances. In [17], a robust feedback linearized controller using upper bound estimation of uncertainties is presented for robot control.

Model-based control systems need an accurate model of the system, which may be extremely hard or even impossible to obtain. Anyway, among the different control algorithms, those methods that have less dependence on the dynamic model and also have less computational load are prioritized. Therefore, the design of a non-model-based control method is more appropriate than the model-based control algorithm.

Several types of research have been conducted on the non-model-based dynamic control method for controlling wheeled mobile robots. In [18], a FLS-based controller is designed to follow the desired path by a two-wheel differential robot. In [19], using a neural network, position control and tracking of the time reference path has been done by a wheeled mobile robot. In [20], tracking of the time reference path has been studied using the non-model-based method of Jacobian matrix. In this method, control signals are produced based on filtered errors.

Although the closed loop system with above mentioned controllers has a good efficiency, the problems of these control methods are as follows:

- The input of these controllers is in the torque space, and in their design, the dynamic equations of wheeled robot drives are not considered.
- In order to guarantee the stability, the input coefficients of the controllers have been adjusted with large values; Therefore, the input of these controllers is not acceptable and their practical implementation is facing problems.
- Due to the use of multiple adaptive rules in the input of these controllers, the volume of control input calculations has increased and in case of a delay in the control input calculation, it is not possible to ensure the stability.

The valuable ability of fuzzy and neural systems in approximating functions has made it possible to design the control system independently of the MR model. FLSs have been used successfully in various control and fault detection problems [21], [22], [23]. When the system is complex and it is not possible to find the optimal solution with analytical methods, intelligent optimization algorithms come into play and make it possible to reach the optimal solution. Recently some FLS based controllers have been designed. For instance, in [24] hybrid approach is presented using T3-FLSs and Bee-Colony algorithm for trajectory tracking in an Autonomous MRs. The performance of different types of FLSs is compared, and the T3-FLS is found to be the best in adapting to uncertainty and achieving better control performance than other systems. In [25], a predictive controller is developed for MRs, and deep learning techniques are employed to improve the tracking accuracy.

In [26], an observer is suggested to identify the modeling error of T3-FLSs, and then fault-tolerant controller is designed. In [27] a methodology is suggested for improving the accuracy of the differential evolution approach in designing an optimal T3-FLS for controlling a MR. The methodology is tested on a type-3 Sugeno controller with different noise levels, and the efficacy is compared to other studies in the literature. A observer-based bounded controller is introduced in [28] for robotic systems with uncertainties, using T3-FLSs to model system uncertainties. A backstepping approach with projection-type laws is utilized, and saturation functions are implemented to prevent actuator constraints from being exceeded. In [29] a fuzzy PID control method is suggested for MRs. The method uses geometric modeling to determine parameters that affect movement accuracy and stability, and combines the superiorities of both PID and FLS-based control. A FLS-based recursive SMC strategy is developed in [30] for an omnidirectional MR used in agriculture. The method uses a kinematic-and-dynamic model to ensure accuracy and stability.

The stability is mathematically studied, and experiments are provided to compare the controller to conventional SMCs. A new controller designed in [31] for an nonholonomic MR that can avoid static and dynamic obstacles while following a desired path. The controller combines a feedback linearization concept and a FLS for path following and obstacle avoidance, respectively. The hybrid controller is proven to converge the robot to the reference path and ensure stability. A finite-time adaptive controller using type-2 FLSs is suggested in [32] for a four-wheels MR using a backstepping technique. The controller uses an T2-FLS based approximator to estimate the complex dynamics and relies only on available parameters. The stability is ensured through finite-time stability theorem, and simulations show its effectiveness compared to an type-1 FLS-based controller and a PID. In [33] the control of a multi-robot systems is discussed. The A T2-FLS based controller using particle swarm optimization is compared with two other algorithms. It is shown that T2-FLSs has better performance in terms of iteration, time, resource usage, and robot movement. In [34] the effectiveness of T2-FLSs in a IoT system is verified by testing in different cars on various roads. In [35] FLSs are used to improve the efficiency in a 6G network.

## B. PROBLEM STATEMENTS AND CONTRIBUTIONS

Previous designs of mobile robot control, are based on the torque control approach. In this strategy, the torque of the robot's joints is the control command or system input. But in practice, the torque command cannot be applied directly to the input of the robot, and it requires the presence of drivers. This strategy ignores the dynamics of engines in the law of control and command execution. This defect questions the efficiency of the robot to perform fast and precise tasks. Furthermore, the torque controller is complicated due to the robot's dynamics. The most problems of the above controllers are summarized as follows:

- Adaptive control is one of the useful methods in controlling nonlinear systems with uncertainty, but this method is only useful in overcoming parameter uncertainties, and in case of non-structural disturbances like friction and un-modeled dynamics, it cannot guarantee the stability.
- In the proposed way of controlling the position of MR and overcoming the existing parameter uncertainties, several adaptive rules have been used in the control input; Therefore, the designed control has a high amount of calculations, and high speed processors should be used in its practical implementation. However, if there is a delay in calculating the control input, the stability of will be violated.

- Traditional FLSs have not enough ability in uncertainty environment. Further researches are required to develop the high-order FLS-based controllers.
- In most of FLS-based controllers, the optimality is not considered.
- Multi-input-multi-output fuzzy rules are been used in the most FLS-based controllers to overcome all uncertainties. Therefore, the number of rules is increased a lot, and the volume of calculations of this controller is also very high.
- In most of methods, many assumptions are considered to derive the stability; Therefore, if one of the assumptions such as the uncertainty limit is not correctly predicted, the guarantee of the stability will be lost.

Regarding the discussion above, the suggested scheme is able to overcome the uncertainties, and intuitive optimization algorithm is used to determine the control input. In this article, an adaptive T3-FLS based control is proposed to ensure the asymptotically stable in the presence of driver dynamics and structural and non-structural uncertainties in the dynamic equations. The main difference between T3-FLSs and conventional FLSs is that T3-FLSs allow for more uncertainty and variability in the data. This is because T3-FLSs use a higher order of membership functions, which can handle more complex and uncertain data. In the proposed control, efforts are made to realize the following advantages:

- The introduced control scheme uses the concept of type-3 FLSs, which proposes a powerful tool to cope with uncertainties. The concept of type-3 FLSs is based on the idea that there are many different levels of uncertainty in under control system. One of the key benefits of using type-3 FLSs in suggested control scheme is that it allows for a much more robust and adaptable approach to managing complex systems. Because the model is designed to handle uncertainty, it is able to cope with a wide range of scenarios and situations. This means that the control scheme is much more effective at dealing with unexpected changes in the MR dynamics.
- The suggested controller uses optimal compensator to ensure the stability and optimal energy usage.
- The controller benefits a stable adaptation rule that guarantees the robot adaptation with unpredicted situations.

## II. PROBLEM FORMULATION

The non-holonomic MRs are considered as [36]:

$$\dot{z}_1 = u_1$$
$$\dot{z}_2 = u_2$$
$$\dot{z}_3 = F(z) + z_2 u_1 + d \qquad (1)$$

where $z = [z_1, z_2, z_3]^T$, and $u_1$, $u_2 \in R$ are control signals. $F(z)$ is a unknown function and $d \in R$ is disturbance. $F(z) + d$ is estimated using the suggested T3-FLS. So, the estimated

system is given as:

$$\dot{z}_1 = u_1$$
$$\dot{z}_2 = u_2$$
$$\dot{z}_3 = \text{T3-FLS}(z) + z_2 u_1 + d \qquad (2)$$

The reference system is defined as:

$$\dot{z}_{1d} = u_{1d}$$
$$\dot{z}_{2d} = u_{2d}$$
$$\dot{z}_{3d} = F(z_d) + z_{2d} u_{1d} \qquad (3)$$

where $z_d = [z_{1d}, z_{2d}, z_{3d}]^T$ denotes the vector of desired states. By defining the error as $z_e = z - z_d$, we have:

$$\dot{z}_{1e} = u_1 - u_{1d}$$
$$\dot{z}_{2e} = u_2 - u_{2d}$$
$$\dot{z}_{3e} = z_{2e} u_{1d} + (z_{2e} + z_{2d})(u_1 - u_{1d})$$
$$\qquad + F(z) - F(z_d) + d \qquad (4)$$

The control signal consists of two parts. The primary controller is the fuzzy SMC and the second part is the optimal compensator. The general diagram of the schemed approach is shown in Fig. 1. The dynamics are fully unknown and are approximated by T3-FLSs. Also, an optimal compensator is used deal with approximation errors and perturbations.
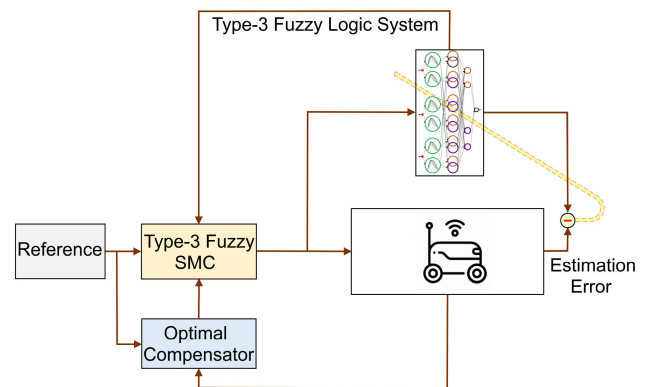


**FIGURE 1.** Control diagram.

So $u_1$ is written as:

$$u_1 = u_{op} + u_2 \qquad (5)$$

$u_{op}$ is the optimal controller and $u_2$ is SMC. The following lemmas and definitions are utilized in stability study. Consider the system (6)

$$\dot{z} = F(z) \qquad (6)$$

if $T > 0$ such that

$$\lim_{t \to T} \|z(t)\| = 0 \qquad (7)$$

for $t \geq T$ we can write $\|z(t)\| = 0$. Since $T > 0$ can bed depended on initial condition $z(0)$, the stability is finite-time.

*Lemma 1:* Suppose that $X$ is subset of $R^n$, we define a dynamic system as $F : X \to X$. It is assumed that

$z_e = 0$ denotes an equilibrium point, and $\upsilon : R^n \to R$ is derivable continuous function such that [37]:

- If $\dot{\upsilon} : R^n \to R$ is semi-negative definite, then $z_e$ is global stable.
- If $\dot{\upsilon}$ is negative definite, then $z_e$ is asymptotic stable.

*Lemma 2:* Consider the system (8) [38],

$$\dot{z} = F(z) + G(z)\,u \qquad (8)$$

such that $z(t) \in R^n$, $u(t) \in R$, $F$ and $G$ are nonlinear vector functions, and $F(0) = 0$. Then, (8) is asymptotic stable, if we have a radial positive definite $\upsilon : R^n \to R$ such that

$$\inf_{u \in R}\left\{ \frac{\partial \upsilon}{\partial z} F(z) + \frac{\partial \upsilon}{\partial z} G(z)\,u \right\} < 0 \qquad \forall z \neq 0 \qquad (9)$$

*Lemma 3:* Consider system $\dot{z} = F(z)$, such that $F$ is derivable on $D = \{\|z\| < r\}$. Suppose that $k$, $\lambda$ and $r_0$ are positive constants and $r_0 < r/k$, then we can write [38]:

$$\|z(t)\| \leq \|z(0)\| ke^{-\lambda t}, \ \forall t \geq 0$$
$$\forall z(0) \in D_0 \qquad (10)$$

such that $D_0 = \{\|z\| < r_0\}$. Then there exist a derivable $\upsilon$ such that

$$c_1 \|z\|^2 \leq \upsilon(z)$$
$$\leq c_2 \|z\|^2$$
$$\frac{\partial \upsilon}{\partial z} F(z) \leq -c_3 \|z\|^2$$
$$\left\| \frac{\partial \upsilon}{\partial z} \right\| \leq c_4 \|z\| \qquad (11)$$

where $z \in D_0$ and $c_i$, $i = 1, .., 4$ are positive constants. If we consider state feedback controller as $u = \Psi(z)$ for (8), then we have:

$$\dot{z} = F(z) + G(z)\,\Psi(z) \qquad (12)$$

and we can derive the stability and write:

$$\frac{\partial \upsilon}{\partial z}[F(z) + G(z)\,\Psi(z)] < 0, \quad \forall z \in D, \quad z \neq 0 \qquad (13)$$

*Lemma 4:* The system (12) with Lyapunov function $\upsilon$ is stable if $\Psi(z)$ is:

$$\Psi(z) = \begin{cases} -\dfrac{\frac{\partial \upsilon}{\partial z} F + \sqrt{\left(\frac{\partial \upsilon}{\partial z} F\right)^2 + \left(\frac{\partial \upsilon}{\partial z} G\right)^4}}{\left(\frac{\partial \upsilon}{\partial z} G\right)} & \text{if } \frac{\partial \upsilon}{\partial z} G \neq 0 \\ 0, & \text{otherwise.} \end{cases}$$

$$(14)$$

where $\Psi(z)$ is a continues function.

## III. TYPE-3 FUZZY LOGIC
The T3-FLS is used as a estimator to enhance the accuracy. The computations are illustrated in below (see Fig. 2).

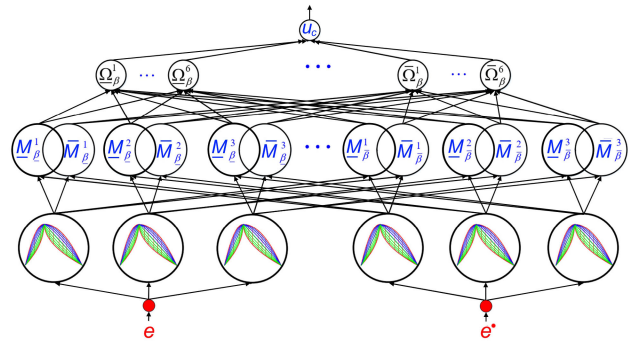1) The inputs are error and it derivative $\mu_1 = e$ and $\mu_2 = \dot{e}$.
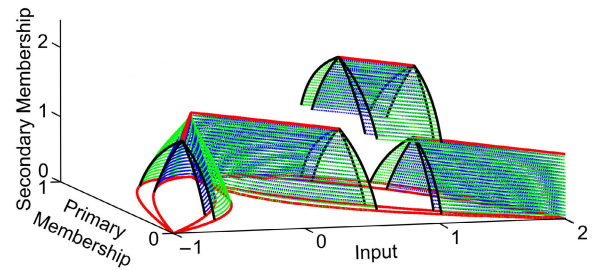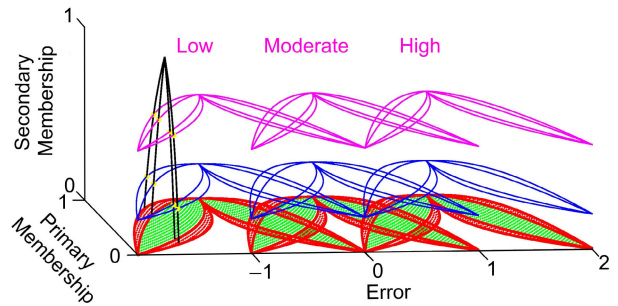


**FIGURE 2.** Type-3 FLS.



**FIGURE 3.** Type-3 MF.



**FIGURE 4.** MFs for error.

2) The memberships $\bar{M}_{\tilde{\Psi}_i^j \,|\,\bar{m}_k}$, $\bar{M}_{\tilde{\Psi}_i^j \,|\,m_k}$, $\underline{M}_{\tilde{\Psi}_i^j \,|\,\bar{m}_k}$, and $\underline{M}_{\tilde{\Psi}_i^j \,|\,m_k}$ for $\tilde{\Psi}_i^j$ ($j$-th membership function (MF) for $\mu_i$, $i = 1, 2$) are computed as (see Fig. 3):

$$\bar{M}_{\tilde{\Psi}_i^j \,|\,\bar{m}_k} =$$

$$\begin{cases} 1 - \left( \dfrac{\left| \mu_i - c_{\tilde{\Psi}_i^j} \right|}{\underline{\vartheta}_{\tilde{\Psi}_i^j}} \right)^{\bar{m}_k} & \text{if } c_{\tilde{\Psi}_i^j} - \underline{\vartheta}_{\tilde{\Psi}_i^j} < \mu_i \leq c_{\tilde{\Psi}_i^j} \\[2mm] 1 - \left( \dfrac{\left| \mu_i - c_{\tilde{\Psi}_i^j} \right|}{\bar{\vartheta}_{\tilde{\Psi}_i^j}} \right)^{\bar{m}_k} & \text{if } c_{\tilde{\Psi}_i^j} < \mu_i \leq c_{\tilde{\Psi}_i^j} + \bar{\vartheta}_{\tilde{\Psi}_i^j} \\[2mm] 0 & \text{if } \mu_i > c_{\tilde{\Psi}_i^j} + \bar{\vartheta}_{\tilde{\Psi}_i^j} \text{ or } \mu_i \leq c_{\tilde{\Psi}_i^j} - \underline{\vartheta}_{\tilde{\Psi}_i^j} \end{cases}$$

$$(15)$$

$$\bar{M}_{\tilde{\Psi}_i^j|_{\underline{m}_k}} =$$

$$\begin{cases} 1 - \left( \dfrac{\left| \mu_i - c_{\tilde{\Psi}_i^j} \right|}{\underline{\vartheta}_{\tilde{\Psi}_i^j}} \right)^{\underline{m}_k} & \text{if } c_{\tilde{\Psi}_i^j} - \underline{\vartheta}_{\tilde{\Psi}_i^j} < \mu_i \leq c_{\tilde{\Psi}_i^j} \\[4mm] 1 - \left( \dfrac{\left| \mu_i - c_{\tilde{\Psi}_i^j} \right|}{\bar{\vartheta}_{\tilde{\Psi}_i^j}} \right)^{\underline{m}_k} & \text{if } c_{\tilde{\Psi}_i^j} < \mu_i \leq c_{\tilde{\Psi}_i^j} + \bar{\vartheta}_{\tilde{\Psi}_i^j} \\[4mm] 0 & \text{if } \mu_i > c_{\tilde{\Psi}_i^j} + \bar{\vartheta}_{\tilde{\Psi}_i^j} \text{ or } \mu_i \leq c_{\tilde{\Psi}_i^j} - \underline{\vartheta}_{\tilde{\Psi}_i^j} \end{cases}$$

(16)

$$\underline{M}_{\tilde{\Psi}_i^j|_{\bar{m}_k}} =$$

$$\begin{cases} 1 - \left( \dfrac{\left| \mu_i - c_{\tilde{\Psi}_i^j} \right|}{\underline{\vartheta}_{\tilde{\Psi}_i^j}} \right)^{\frac{1}{\bar{m}_k}} & \text{if } c_{\tilde{\Psi}_i^j} - \underline{\vartheta}_{\tilde{\Psi}_i^j} < \mu_i \leq c_{\tilde{\Psi}_i^j} \\[4mm] 1 - \left( \dfrac{\left| \mu_i - c_{\tilde{\Psi}_i^j} \right|}{\bar{\vartheta}_{\tilde{\Psi}_i^j}} \right)^{\frac{1}{\bar{m}_k}} & \text{if } c_{\tilde{\Psi}_i^j} < \mu_i \leq c_{\tilde{\Psi}_i^j} + \bar{\vartheta}_{\tilde{\Psi}_i^j} \\[4mm] 0 & \text{if } \mu_i > c_{\tilde{\Psi}_i^j} + \bar{\vartheta}_{\tilde{\Psi}_i^j} \text{ or } \mu_i \leq c_{\tilde{\Psi}_i^j} - \underline{\vartheta}_{\tilde{\Psi}_i^j} \end{cases}$$

(17)

$$\underline{M}_{\tilde{\Psi}_i^j|_{\underline{m}_k}} =$$

$$\begin{cases} 1 - \left( \dfrac{\left| \mu_i - c_{\tilde{\Psi}_i^j} \right|}{\underline{\vartheta}_{\tilde{\Psi}_i^j}} \right)^{\frac{1}{\underline{m}_k}} & \text{if } c_{\tilde{\Psi}_i^j} - \underline{\vartheta}_{\tilde{\Psi}_i^j} < \mu_i \leq c_{\tilde{\Psi}_i^j} \\[4mm] 1 - \left( \dfrac{\left| \mu_i - c_{\tilde{\Psi}_i^j} \right|}{\bar{\vartheta}_{\tilde{\Psi}_i^j}} \right)^{\frac{1}{\underline{m}_k}} & \text{if } c_{\tilde{\Psi}_i^j} < \mu_i \leq c_{\tilde{\Psi}_i^j} + \bar{\vartheta}_{\tilde{\Psi}_i^j} \\[4mm] 0 & \text{if } \mu_i > c_{\tilde{\Psi}_i^j} + \bar{\vartheta}_{\tilde{\Psi}_i^j} \text{ or } \mu_i \leq c_{\tilde{\Psi}_i^j} - \underline{\vartheta}_{\tilde{\Psi}_i^j} \end{cases}$$

(18)

where $\bar{m}_k/\underline{m}_k$ denotes the upper/lower horizontal slice.

3) The $l$-th rule firings $\bar{\Omega}_{\bar{m}_k}^l$, $\bar{\Omega}_{\underline{m}_k}^l$, $\underline{\Omega}_{\bar{m}_k}^l$, and $\underline{\Omega}_{\underline{m}_k}^l$ are written as

$$\bar{\Omega}_{\bar{m}_k}^l = \bar{M}_{\tilde{\Psi}_1^{q_1}|_{\bar{m}_k}} \cdot \bar{M}_{\tilde{\Psi}_1^{q_2}|_{\bar{m}_k}} \cdots \bar{M}_{\tilde{\Psi}_1^{q_n}|_{\bar{m}_k}}$$

(19)

$$\bar{\Omega}_{\underline{m}_k}^l = \bar{M}_{\tilde{\Psi}_1^{q_1}|_{\underline{m}_k}} \cdot \bar{M}_{\tilde{\Psi}_1^{q_2}|_{\underline{m}_k}} \cdots \bar{M}_{\tilde{\Psi}_1^{q_n}|_{\underline{m}_k}}$$

(20)

$$\underline{\Omega}_{\bar{m}_k}^l = \underline{M}_{\tilde{\Psi}_1^{q_1}|_{\bar{m}_k}} \cdot \underline{M}_{\tilde{\Psi}_1^{q_2}|_{\bar{m}_k}} \cdots \underline{M}_{\tilde{\Psi}_1^{q_n}|_{\bar{m}_k}}$$

(21)

$$\underline{\Omega}_{\underline{m}_k}^l = \underline{M}_{\tilde{\Psi}_1^{q_1}|_{\underline{m}_k}} \cdot \underline{M}_{\tilde{\Psi}_1^{q_2}|_{\underline{m}_k}} \cdots \underline{M}_{\tilde{\Psi}_1^{q_n}|_{\underline{m}_k}}$$

(22)

4) The output of T3-FLS is given as:

$$\text{T3-FLS} = \sum_{k=1}^{K} \left( \underline{m}_k \underline{F}_k + \bar{m}_k \bar{F}_k \right) \bigg/ \sum_{k=1}^{K} \left( \underline{m}_k + \bar{m}_k \right)$$

(23)

where,

$$\bar{F}_k = \frac{\sum_{l=1}^{M} \left( \bar{\Omega}_{\bar{m}_k}^l \bar{w}_l + \underline{\Omega}_{\bar{m}_k}^l \underline{w}_l \right)}{\sum_{l=1}^{M} \left( \bar{\Omega}_{\bar{m}_k}^l + \underline{\Omega}_{\bar{m}_k}^l \right)}$$

(24)

$$\underline{F}_k = \frac{\sum_{l=1}^{M} \left( \bar{\Omega}_{\underline{m}_k}^l \bar{w}_l + \underline{\Omega}_{\underline{m}_k}^l \underline{w}_l \right)}{\sum_{l=1}^{M} \left( \bar{\Omega}_{\underline{m}_k}^l + \underline{\Omega}_{\underline{m}_k}^l \right)}$$

(25)

The MFs of error and derivative of error are illustrated in Figs. 4 and 5, respectively. The rules paterers are adjusted as follows:

$$\bar{w}_l(t+1) = \bar{w}_l(t) + \frac{1}{\sum_{k=1}^{K} \left( \underline{m}_k + \bar{m}_k \right)} \sum_{k=1}^{K} \frac{\bar{m}_k \bar{\Omega}_{\bar{m}_k}^l}{\sum_{l=1}^{M} \left( \bar{\Omega}_{\bar{m}_k}^l + \underline{\Omega}_{\bar{m}_k}^l \right)}$$

$$+ \frac{1}{\sum_{k=1}^{K} \left( \underline{m}_k + \bar{m}_k \right)} \sum_{k=1}^{K} \frac{\underline{m}_k \bar{\Omega}_{\underline{m}_k}^l}{\sum_{l=1}^{M} \left( \bar{\Omega}_{\underline{m}_k}^l + \underline{\Omega}_{\underline{m}_k}^l \right)}$$

$$\underline{w}_l(t+1) = \underline{w}_l(t) + \frac{1}{\sum_{k=1}^{K} \left( \underline{m}_k + \bar{m}_k \right)} \sum_{k=1}^{K} \frac{\bar{m}_k \underline{\Omega}_{\bar{m}_k}^l}{\sum_{l=1}^{M} \left( \bar{\Omega}_{\bar{m}_k}^l + \underline{\Omega}_{\bar{m}_k}^l \right)}$$

$$+ \frac{1}{\sum_{k=1}^{K} \left( \underline{m}_k + \bar{m}_k \right)} \sum_{k=1}^{K} \frac{\underline{m}_k \underline{\Omega}_{\underline{m}_k}^l}{\sum_{l=1}^{M} \left( \bar{\Omega}_{\underline{m}_k}^l + \underline{\Omega}_{\underline{m}_k}^l \right)}$$
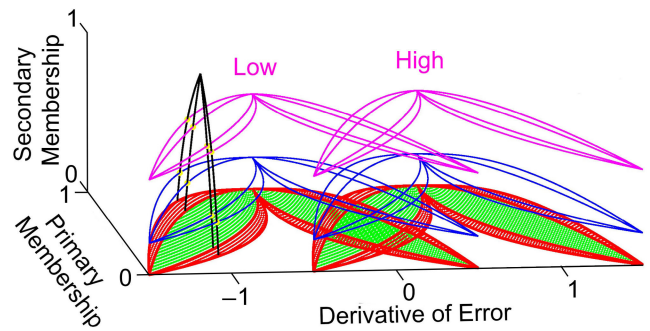


**FIGURE 5.** MFs for derivative of error.

## IV. CONTROL DESIGN

The optimal controller is designed such that (26) is minimized:

$$V = \int_0^{\infty} \left( q(z) + u_{op}^2 \right) dt$$

(26)

where $q(z)$ is a semi-definite constant, and we have

$$\dot{z}_3 = \text{T3-FLS}(z) + z_2 u_{op}$$

(27)

where $z \in R^3$ represent the vector of states, T3-FLS$(z)$ is the estimation of nonlinear function. A Lyapunov function is considered as $\upsilon_1$. Then we can write:

$$\dot{\upsilon}_1 = \frac{\partial \upsilon_1}{\partial z} \dot{z} = L_F \upsilon_1 + L_{z_2} \upsilon_1 u_{op}$$

(28)

where $L_F \upsilon_1 = \frac{\partial \upsilon_1}{\partial z} F$, and $L_{z_2} \upsilon_1 = \frac{\partial \upsilon_1}{\partial z} z_2$. $L$ denotes the Lie derivative operator. By the use of Lemma 4 it is concluded that if (27) is stabilizable, then there is a candidate Lyapunov function. The controller is considered as

$$u_{op} =$$

$$
\begin{cases}
- \left( \dfrac{a\,(z) \, + \, \sqrt{a\,(z)^2 \, + \, q\,(z)\, b\,(z)^T b\,(z)}}{b\,(z)^T b\,(z)} \right) b\,(z)^T, & b(z) \neq 0 \\[4mm]
0, & b(z) = 0
\end{cases}
$$

$$(29)$$

where

$$a\,(z) = L_F\,\upsilon_1, \tag{30}$$
$$b\,(z) = L_{z_2}\,\upsilon_1 \tag{31}$$

To find the controller we need to solve the Hamilton-Jacobi-Bellman relation:

$$L_F \upsilon_1{}^* - \frac{1}{4} (L_{z_2} \upsilon_1{}^*)^T L_{z_2}\, \upsilon_1{}^* + q\,(z) = 0 \tag{32}$$

where $\upsilon_1{}^*$ is the optimal solution and is defined as:

$$\upsilon_1{}^* = \inf_{u_{op}} \int_t^\infty \left( q\,(z) \, + \, u_{op}{}^2 \right) d\tau \tag{33}$$

Then $u^*$ is considered as:

$$u^* = -\frac{1}{2} L_{z_2}\, \upsilon_1{}^* \tag{34}$$

Consider a scalar as $\lambda$ such that $\upsilon_1{}^* = \lambda \upsilon_1$, then $u^*$ is written as:

$$u^* = -\frac{1}{2} (\lambda\, L_{z_2}\, \upsilon_1)^T \tag{35}$$

By replacing $\upsilon_1{}^* = \lambda \upsilon_1$ in (32), we have:

$$\lambda\, L_F \upsilon_1 - \frac{1}{4} \lambda^2 (L_{z_2}\,\upsilon_1)^T L_{z_2}\, \upsilon_1 + q\,(z) = 0 \tag{36}$$

By solving (36) and using (30) and (31), $\lambda$ is obtained as:

$$\lambda = 2 \left( \frac{a\,(z) \, + \, \sqrt{a\,(z)^2 \, + \, q\,(z)\, b\,(z)^T b\,(z)}}{b\,(z)^T b\,(z)} \right) \tag{37}$$

Replacing $\lambda$ in (35) yields:

$$u^* = - \left( \frac{a\,(z) \, + \, \sqrt{a\,(z)^2 \, + \, q\,(z)\, b\,(z)^T b\,(z)}}{b\,(z)^T b\,(z)} \right) b\,(z)^T \tag{38}$$

Considering (28) and (29) and the fact that $L_F \upsilon_1 < 0$ for $L_{z_2} \upsilon_1 = 0$, we can obtain $\dot{\upsilon}_1 < 0$ for $u_{op} = 0$. On the other hand, for $u_{op} \neq 0$, we can write:

$$\dot{\upsilon}_1 = -\sqrt{b\,(z)^2 q\,(z) + a\,(z)^2} < 0 \tag{39}$$

Then, it is proved that the controller (29) minimizes (26), and so the system is stable.

## V. COMPENSATOR

To eliminate the effect of estimation errors, a compensator is added to the designed optimal controller. Consider the following sliding surfaces:

$$\sigma_1 = z_{2e} + z_{3e} = 0$$
$$\sigma_2 = \dot{\sigma}_1 + \rho_1 \sigma_1{}^{q_1/p_1} = 0$$
$$\sigma_3 = \dot{\sigma}_2 + \rho_2 \sigma_2{}^{q_2/p_2} = 0 \tag{40}$$

where $q_i$ and $p_i$ are positive and $q_i < p_i$. For sliding surface $\sigma_i$, we can write:

$$\dot{\sigma}_1 = \dot{z}_{2e} + \dot{z}_{3e}$$

$$= u_2 - u_{2d} + z_{2e}\, u_{1d} + \text{T3-FLS}\,(z) - F(z_d)$$

$$\dot{\sigma}_2 = \ddot{\sigma}_1 + \rho_1 \frac{d}{dt} \left( \sigma_1{}^{q_1/p_1} \right)$$

$$\dot{\sigma}_3 = \ddot{\sigma}_2 + \rho_2 \frac{d}{dt} \left( \sigma_2{}^{q_2/p_2} \right) \tag{41}$$

The switching criteria is defined as:

$$\dot{\sigma}_1 < -\rho\, sgn\,(\sigma_1) \tag{42}$$

where $\rho > 0$ and $sgn(\sigma_1)$ is:

$$
sgn\,(\sigma_1) =
\begin{cases}
1, & \sigma_1 > 0 \\
0, & \sigma_1 = 0 \\
-1, & \sigma_1 < 0
\end{cases}
\tag{43}
$$

Then from (41) and 42, we will have:

$$u_2 < u_{2d} - z_{2e} u_{1d} - \text{T3-FLS}\,(z) + F(z_d) - \rho\, sgn(\sigma_1) \tag{44}$$

To remove the chattering of control signal, we modify the sliding surface $\sigma_1$ as:

$$\kappa = \sigma_1 + \delta\, \dot{\sigma}_1{}^{s/m} \tag{45}$$

where $1 < \frac{s}{m} < 2$, $\delta$ is the switching gain. Then, (41) is rewritten as:

$$\dot{\sigma}_1 = u_2 - u_{2d} + z_{2e} u_{1d} + \text{T3-FLS}\,(z) - F(z_d)$$
$$= u_2 + \zeta. \tag{46}$$

From (45), we have:

$$\dot{\kappa} = -\eta_1\, sgn\,(\kappa) - \varepsilon_1 \kappa \tag{47}$$

where $\varepsilon_1 > 0$ $\eta_1 > 0$, and we can write:

$$\dot{\kappa} = \dot{\sigma}_1 + \delta \frac{s}{m} \dot{\sigma}_1{}^{s/m-1} \ddot{\sigma}_1$$
$$= \delta \frac{s}{m} \dot{\sigma}_1{}^{s/m-1} \left( \frac{m}{\delta s} \dot{\sigma}_1{}^{2-s/m} + \ddot{\sigma}_1 \right) \tag{48}$$

For $s$ and $m$, we can write:

$$\dot{\sigma}_1{}^{s/m-1} > 0, \ \dot{\sigma}_1 \neq 0$$
$$\dot{\sigma}_1{}^{s/m-1} = 0, \ \dot{\sigma}_1 = 0 \tag{49}$$

Considering $\delta\,(s/m)\dot{\sigma}_1{}^{s/m-1}$ in (48), and considering $\eta_2 > 0$ for $\dot{\sigma}_1 \neq 0$, we have:

$$\dot{\kappa} = \eta_2 \left( \frac{m}{\delta s} \dot{\sigma}_1{}^{2-s/m} + \ddot{\sigma}_1 \right) \tag{50}$$

From (47) and (50), we can write:

$$\frac{m}{\delta s} \dot{\sigma}_1{}^{2-s/m} + \ddot{\sigma}_1 = -\eta\, sgn\,(\kappa) - \varepsilon\kappa \tag{51}$$

where $\eta = \eta_1/\eta_2 > 0$ and $\varepsilon = \varepsilon/\eta_2 > 0$. From (51) we can write:

$$\ddot{\sigma}_1 = -\eta\, sgn\,(\kappa) - \varepsilon\kappa - \frac{m}{\delta s} \dot{\sigma}_1{}^{2-s/m} \tag{52}$$

By time derivative of (46), we have:

$$\ddot{\sigma}_1 = \dot{u}_2 + \dot{\zeta} \tag{53}$$

Then, from (52) and (53), the compensator is give as:

$$u_2 = -\int_0^t \left[ \eta\, sgn\,(\kappa) + \varepsilon\kappa + \frac{m}{\delta s}\dot{\sigma}_1{}^{2-s/m} + \dot{\zeta} \right] d\tau \tag{54}$$

*Theorem 1:* Considering the sliding surface as (45), the compensator as (54), and the controller as (55), the asymptotically stability is ensured.

$$u_1 = u_{op} + u_2 \tag{55}$$

**Proof.** Consider the Lyapunov function as:

$$\upsilon_2 = \frac{1}{2}\kappa^2 \tag{56}$$

By taking the time derivative we have:

$$\dot{\upsilon}_2 = \kappa\dot{\kappa} \tag{57}$$

By the use of (48), (53), and (57), we have:

$$\dot{\upsilon}_2 = \kappa \left[ \dot{\sigma}_1 + \frac{s\delta}{m} \dot{\sigma}_1{}^{s/m-1}\ddot{\sigma}_1 \right]$$
$$= \kappa \left[ \dot{\sigma}_1 + \frac{s\delta}{m} \dot{\sigma}_1{}^{s/s/m-1}(\dot{u}_2 + \dot{\zeta}) \right] \tag{58}$$

From (54), we can rewrite (58) as:

$$\dot{\upsilon}_2 = \kappa\dot{\sigma}_1 + \kappa\frac{s\delta}{m}\dot{\sigma}_1{}^{s/m-1}$$
$$\times \left( -\eta\, sgn\,(\kappa) - \varepsilon\kappa - \frac{m}{\delta s}\dot{\sigma}_1{}^{2-s/m} - \dot{\zeta} + \dot{\zeta} \right)$$
$$= \kappa \left[ \frac{s\delta}{m}\dot{\sigma}_1{}^{s/m-1}(-\eta\, sgn\,(\kappa) - \varepsilon\kappa) \right]$$
$$= \frac{s\delta}{m}\dot{\sigma}_1{}^{s/m-1}\left[ -\eta|\kappa| - \varepsilon\kappa^2 \right]. \tag{59}$$

If $\delta > 0$ and $1 < s/m < 2$, it is concluded that for $\dot{\sigma}_1 \neq 0$ and $\dot{\sigma}_1{}^{s/m-1} = 0$, we have $\dot{\sigma}_1{}^{s/m-1} > 0$. Then form (59), we can write:

$$\dot{\upsilon}_2(\kappa) \leq -\left[ \eta|\kappa| + |\kappa|^2\varepsilon \right]\eta_2$$
$$= -\upsilon(\kappa)^{\bar{\eta}}\bar{m} - \upsilon(\kappa)\bar{s} \leq 0 \tag{60}$$

where $\bar{\eta} = 1/2$, $\bar{s} = 2\eta_2\varepsilon$ and $\bar{m} = \sqrt{2}\eta_2\eta$. Then the sliding surface $\kappa$ is converged to zero.

## VI. SIMULATION

The following case-study system is considered:

$$\begin{aligned} \dot{z}_1 &= u_1 \\ \dot{z}_2 &= u_2 \\ \dot{z}_3 &= z_1 + z_2^2 + z_3 + z_2 u_1 + \sin(0.1\pi t) \end{aligned} \tag{61}$$

where $F(z) = z_1 + z_2^2 + z_3$ and $d = \sin(0.1\pi t)$. The dynamics of $z_{1d}$, $z_{2d}$, and $z_{3d}$ are considered as follows:

$$\begin{aligned} \dot{z}_{1d} &= u_{1d} \\ \dot{z}_{2d} &= u_{2d} \\ \dot{z}_{3d} &= F\,(z_d) + z_{2d}u_{1\,d} \end{aligned} \tag{62}$$

where $F(z_d) = z_{1d} + z_{2d}^2 + z_{3d}$, $z_{ie} = z_i - z_{id}$ ($i = 1, 2, 3$). The simulation condition is given in Table 1. The error dynamics are given as:

$$\begin{aligned} \dot{z}_{1e} &= u_1 - u_{1d} \\ \dot{z}_{2e} &= u_2 - u_{2d} \\ \dot{z}_{3e} &= z_{2e}u_{1d} + (z_2)(u_1 - u_{1d}) + F(z) - F(z_d) + d \end{aligned} \tag{63}$$

The optimal controller is written as:

$$u_{op} = \begin{cases} -z_1 - z_2 z_3 - \dfrac{z_1 + z_2 + z_3 + \sqrt{\phi}}{\Gamma - 2}, & \Gamma \neq 0 \\ 0, & \Gamma = 0 \end{cases} \tag{64}$$

where $\phi = z_2 + z_3$ and $\Gamma = 5z_1 + 2(z_2 + z_3)$.

**TABLE 1.** Simulation parameters.

| Parameters | Values |
|:---:|:---:|
| $s$ | 2 |
| $\rho_2$ | 1 |
| $\rho_1$ | 1 |
| $\eta$ | 0.1 |
| $P_1$ | 1 |
| $P_2$ | 5 |
| $\varepsilon$ | 0.001 |
| $m$ | 1 |
| $\mu$ | 0.1 |
| $\kappa$ | 0.001 |
| $z_e(0)$ | [1, 0, 1] |
| $u_1(0)$ | $-5$ |
| $u_2(0)$ | $-1$ |
| $u_{1d}(0)$ | $\exp\left(-5t\right)$ |
| $u_{2d}(0)$ | $\exp\left(-2t\right)$ |

The provided figures offer a comprehensive overview of the performance. Figure 6 depicts the error trajectories of $z_{1e}$, $z_{2e}$, and $z_{3e}$, crucial in evaluating the effectiveness of the control approach. It is observed that these error trajectories reach zero level in a short amount of time, indicating a robust and excellent control performance. The control trajectories, illustrated in Fig. 7(a)–(b), showcase

the implementable signals with no chattering phenomenon, a desirable characteristic of a stable control process. The smooth and stable control process is further emphasized by the optimal control trajectory depicted in Fig. 7(c), where soft control inputs are utilized to overcome the nonlinearities and disturbances present in the system.
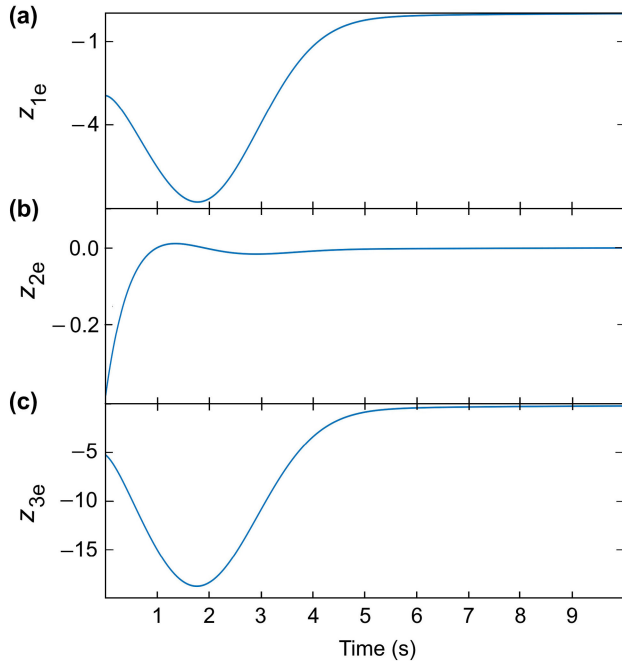


**FIGURE 6.** Trajectories of (a) $z_{1e}$, (b) $z_{1e}$, and (c) $z_{3e}$.

Furthermore, the trajectories of $\sigma_1$, $\sigma_2$ and $\sigma_3$ are shown in Fig. 8, which provides insight into the convergence of the sliding surfaces to zero level. Convergence of these sliding surfaces to zero highlights the effectiveness of the control approach in achieving the desired system response. Overall, the provided figures demonstrate the successful implementation of the control strategy, resulting in a stable and accurate system response. The absence of chattering phenomenon and fast convergence to zero error indicate that the control approach is robust and effective, making it suitable for practical applications.

In addition to the aforementioned figures, the performance of the control approach can also be evaluated by analyzing the control effort required to achieve the desired system response. Figure 8 illustrates the control effort required for each input signal to achieve the desired trajectory. It is observed that the control effort is minimal and remains within a reasonable range, indicating that the control approach is energy-efficient and practical.

Moreover, the robustness of the control approach can be evaluated by analyzing the response of the system to external disturbances. It is observed that the control approach quickly compensates for the disturbance and restores the system to its desired trajectory. This highlights the robustness of the
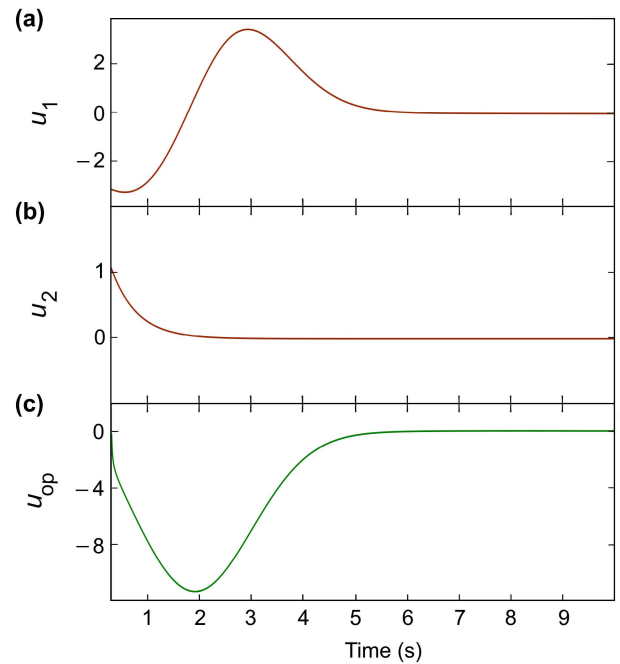


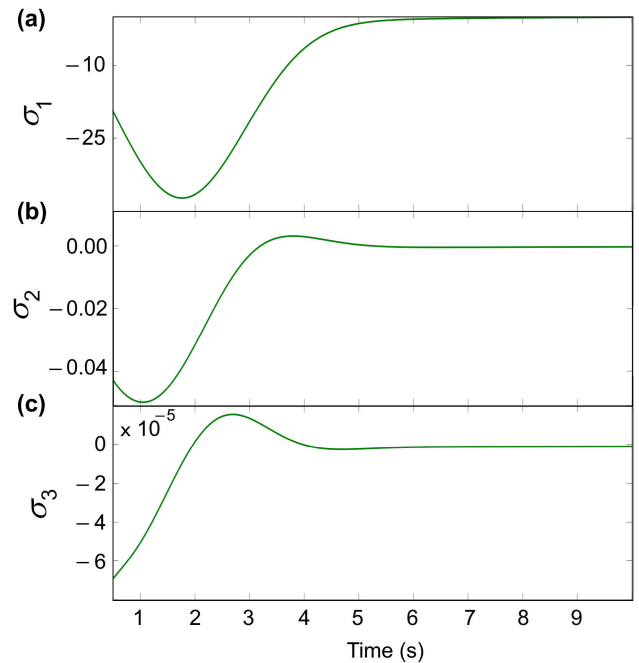**FIGURE 7.** Trajectories of (a) $u_1$, (b) $u_2$, and (c) $u_{op}$.



**FIGURE 8.** Trajectories of (a) $\sigma_1$, (b) $\sigma_2$, and (c) $\sigma_3$.

control approach in dealing with external disturbances, which is a desirable characteristic for practical applications.

To better show the capabilities of T3-FLSs, a comparison is conducted with other types of FLSs. The aim of this comparison is to determine whether T3-FLSs are superior in dealing with uncertainty in real-world applications. We add a noise to the dynamics to better evaluate the efficacy.

The results of comparison are presented in Table 2, which clearly shows that the use of T3-FLSs improves accuracy in the presence of noise. This is particularly evident in highly noisy conditions, where type-3 fuzzy systems outperform other types of fuzzy systems.

**TABLE 2. Comparison of RMSE.**

| Noise Variance | Type of FLS | | |
|---|---|---|---|
| | 1 | 2 | 3 |
| 0 | 0.2653 | 0.2570 | 0.1407 |
| 0.05 | 1.4714 | 1.0421 | 0.3217 |
| 0.1 | 7.1021 | 3.8156 | 0.5301 |

## VII. CONCLUSION

In this study, the control of third-order non-holonomic MRs was investigated. A new approach based on T3-FLSs was introduced to deal with the uncertain dynamics of MR and unpredictable perturbations. In order to eliminate the external disturbances affecting the system, an integral optimal controller was designed. By designing the optimal control law and solving the HJB equations, it was shown that the performance index is minimized. By Lyapunov analysis, it was proved that the sliding surfaces were converged to zero in a limited time and to keep the system on the sliding surface. The provided simulation results show a comprehensive evaluation of performance. The fast convergence to zero error, absence of chattering phenomenon, minimal control effort, and robustness to external disturbances verify the effectiveness and practicality of the control approach. These results are promising for practical applications in various fields, including aerospace, robotics, and industrial automation.

## REFERENCES

[1] B. M. Yousuf, A. S. Khan, and S. M. Khan, "Dynamic modeling and tracking for nonholonomic mobile robot using PID and back-stepping," *Adv. Control Appl.*, vol. 3, no. 3, p. e71, Sep. 2021.

[2] F. Chen, X. Qiu, K. A. Alattas, A. Mohammadzadeh, and E. Ghaderpour, "A new fuzzy robust control for linear parameter-varying systems," *Mathematics*, vol. 10, no. 18, p. 3319, Sep. 2022.

[3] A. Kumar, R. Raj, A. Kumar, and B. Verma, "Design of a novel mixed interval type-2 fuzzy logic controller for 2-DOF robot manipulator with payload," *Eng. Appl. Artif. Intell.*, vol. 123, Aug. 2023, Art. no. 106329.

[4] A. Al-Mahturi, F. Santoso, M. A. Garratt, and S. G. Anavatti, "A novel evolving type-2 fuzzy system for controlling a mobile robot under large uncertainties," *Robotics*, vol. 12, no. 2, p. 40, Mar. 2023.

[5] J. Huang, M. Zhang, and T. Fukuda, "Interval type-2 fuzzy logic control of mobile wheeled inverted pendulums," in *Robust and Intelligent Control of a Typical Underactuated Robot: Mobile Wheeled Inverted Pendulum.* Singapore: Springer, 2023, pp. 79–95.

[6] Z. Jing, Q. Xu, and J. Huang, "A review on kinematic analysis and dynamic stable control of space flexible manipulators," *Aerosp. Syst.*, vol. 2, pp. 1–14, Aug. 2019.

[7] W. Benchouche, R. Mellah, and M. S. Bennouna, "The impact of the dynamic model in feedback linearization trajectory tracking of a mobile robot," *Periodica Polytechnica Electr. Eng. Comput. Sci.*, vol. 65, no. 4, pp. 329–343, Oct. 2021.

[8] H. Batti, C. B. Jabeur, and H. Seddik, "Autonomous smart robot for path predicting and finding in maze based on fuzzy and neuro-fuzzy approaches," *Asian J. Control*, vol. 23, no. 1, pp. 3–12, Jan. 2021.

[9] N. T. Binh, N. A. Tung, D. P. Nam, and N. H. Quang, "An adaptive backstepping trajectory tracking control of a tractor trailer wheeled mobile robot," *Int. J. Control, Autom. Syst.*, vol. 17, no. 2, pp. 465–473, Feb. 2019.

[10] Z. Chen, Y. Liu, W. He, H. Qiao, and H. Ji, "Adaptive-neural-network-based trajectory tracking control for a nonholonomic wheeled mobile robot with velocity constraints," *IEEE Trans. Ind. Electron.*, vol. 68, no. 6, pp. 5057–5067, Jun. 2021.

[11] A. Štefek, V. T. Pham, V. Krivanek, and K. L. Pham, "Optimization of fuzzy logic controller used for a differential drive wheeled mobile robot," *Appl. Sci.*, vol. 11, no. 13, p. 6023, Jun. 2021.

[12] J. Guo, C. Li, and S. Guo, "A novel step optimal path planning algorithm for the spherical mobile robot based on fuzzy control," *IEEE Access*, vol. 8, pp. 1394–1405, 2020.

[13] J. Han, X. Liu, X. Wei, and X. Hu, "Adaptive adjustable dimension observer based fault estimation for switched fuzzy systems with unmeasurable premise variables," *Fuzzy Sets Syst.*, vol. 452, pp. 149–167, Jan. 2023.

[14] K. Singhal, V. Kumar, and K. P. S. Rana, "Robust trajectory tracking control of non-holonomic wheeled mobile robots using an adaptive fractional order parallel fuzzy PID controller," *J. Franklin Inst.*, vol. 359, no. 9, pp. 4160–4215, Jun. 2022.

[15] M. Cui, H. Liu, X. Wang, and W. Liu, "Adaptive control for simultaneous tracking and stabilization of wheeled mobile robot with uncertainties," *J. Intell. Robotic Syst.*, vol. 108, no. 3, p. 46, Jul. 2023.

[16] H. R. Shafei and M. Bahrami, "Trajectory tracking control of a wheeled mobile robot in the presence of matched uncertainties via a composite control approach," *Asian J. Control*, vol. 23, no. 6, pp. 2805–2823, Nov. 2021.

[17] V. Sumathy and D. Ghose, "Robust adaptive feedback linearization controller for an aerial robot working in narrow corridor and in-door environments," in *Proc. Int. Symp. Asian Control Assoc. Intell. Robot. Ind. Autom. (IRIA)*, Sep. 2021, pp. 419–425.

[18] J. Simon, "Fuzzy control of self-balancing, two-wheel-driven, SLAM-based, unmanned system for Agriculture 4.0 applications," *Machines*, vol. 11, no. 4, p. 467, Apr. 2023.

[19] J. Li, Q. Wu, J. Wang, and J. Li, "Neural networks-based sliding mode tracking control for the four wheel-legged robot under uncertain interaction," *Int. J. Robust Nonlinear Control*, vol. 31, no. 9, pp. 4306–4323, Jun. 2021.

[20] I. Agustian, N. Daratha, R. Faurina, A. Suandi, and Sulistyaningsih, "Robot manipulator control with inverse kinematics PD-pseudoinverse Jacobian and forward kinematics Denavit Hartenberg," 2021, *arXiv:2103.10461*.

[21] J. Han, X. Liu, X. Xie, and X. Wei, "Dynamic output feedback fault tolerant control for switched fuzzy systems with fast time varying and unbounded faults," *IEEE Trans. Fuzzy Syst.*, vol. 31, no. 9, pp. 3185–3196, Sep. 2023.

[22] M. A. Khaniki, M. Manthouri, and M. A. Khanesar, "Adaptive non-singular fast terminal sliding mode control and synchronization of a chaotic system via interval type-2 fuzzy inference system with proportionate controller," *Iranian J. Fuzzy Syst.*, May 2023, Art. no. 7625, doi: 10.22111/ijfs.2023.7625.

[23] J. Han, H. Zhang, X. Liu, and X. Wei, "Dissipativity-based fault detection for uncertain switched fuzzy systems with unmeasurable premise variables," *IEEE Trans. Fuzzy Syst.*, vol. 27, no. 12, pp. 2421–2432, Dec. 2019.

[24] L. Amador-Angulo, O. Castillo, P. Melin, and J. R. Castro, "Interval type-3 fuzzy adaptation of the bee colony optimization algorithm for optimal fuzzy control of an autonomous mobile robot," *Micromachines*, vol. 13, no. 9, p. 1490, Sep. 2022.

[25] A. S. Alkabaa, O. Taylan, M. Balubaid, C. Zhang, and A. Mohammadzadeh, "A practical type-3 fuzzy control for mobile robots: Predictive and Boltzmann-based learning," *Complex Intell. Syst.*, vol. 9, no. 6, pp. 6509–6522, Dec. 2023.

[26] H. Bie, P. Li, F. Chen, and E. Ghaderpour, "An observer-based type-3 fuzzy control for non-holonomic wheeled robots," *Symmetry*, vol. 15, no. 7, p. 1354, Jul. 2023.

[27] C. Peraza, P. Ochoa, O. Castillo, and Z. W. Geem, "Interval-type 3 fuzzy differential evolution for designing an Interval-type 3 fuzzy controller of a unicycle mobile robot," *Mathematics*, vol. 10, no. 19, p. 3533, Sep. 2022.

[28] O. Elhaki, K. Shojaei, A. Mohammadzadeh, and S. Rathinasamy, "Robust amplitude-limited interval type-3 neuro-fuzzy controller for robot manipulators with prescribed performance by output feedback," *Neural Comput. Appl.*, Dec. 2022.

[29] G. Cao, X. Zhao, C. Ye, S. Yu, B. Li, and C. Jiang, "Fuzzy adaptive PID control method for multi-mecanum-wheeled mobile robot," *J. Mech. Sci. Technol.*, vol. 36, no. 4, pp. 2019–2029, Apr. 2022.

[30] Z. Sun, S. Hu, H. Xie, H. Li, J. Zheng, and B. Chen, "Fuzzy adaptive recursive terminal sliding mode control for an agricultural omnidirectional mobile robot," *Comput. Electr. Eng.*, vol. 105, Jan. 2023, Art. no. 108529.

[31] S. Mondal, R. Ray, S. N. Reddy, and S. Nandy, "Intelligent controller for nonholonomic wheeled mobile robot: A fuzzy path following combination," *Math. Comput. Simul.*, vol. 193, pp. 533–555, Mar. 2022.

[32] X. Zou, T. Zhao, and S. Dian, "Finite-time adaptive interval type-2 fuzzy tracking control for mecanum-wheel mobile robots," *Int. J. Fuzzy Syst.*, vol. 24, no. 3, pp. 1570–1585, Apr. 2022.

[33] A. Islami, S. Nurmaini, and H. Satria, "Comparative analysis multi-robot formation control modeling using fuzzy logic type 2—Particle swarm optimization," *Comput. Eng. Appl. J.*, vol. 11, no. 3, pp. 167–176, Oct. 2022.

[34] M. Woźniak, A. Zielonka, and A. Sikora, "Driving support by type-2 fuzzy logic control model," *Expert Syst. Appl.*, vol. 207, Nov. 2022, Art. no. 117798.

[35] M. Wozniak, A. Zielonka, A. Sikora, Md. J. Piran, and A. Alamri, "6G-enabled IoT home environment control using fuzzy rules," *IEEE Internet Things J.*, vol. 8, no. 7, pp. 5442–5452, Apr. 2021.

[36] Y.-P. Tian and K.-C. Cao, "Time-varying linear controllers for exponential tracking of non-holonomic systems in chained form," *Int. J. Robust Nonlinear Control*, vol. 17, no. 7, pp. 631–647, 2007.

[37] R. Jafari, A. Kable, and M. Hagan, "Forward and converse Lyapunov theorems for discrete dynamical systems," *IEEE Trans. Autom. Control*, vol. 59, no. 9, pp. 2496–2501, Sep. 2014.

[38] F. Mazenc and M. Malisoff, "Control-Lyapunov functions for systems satisfying the conditions of the Jurdjevic–Quinn theorem," in *Proc. 44th IEEE Conf. Decis. Control*, Mali, 2005, pp. 4724–4729.
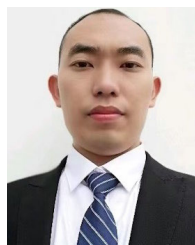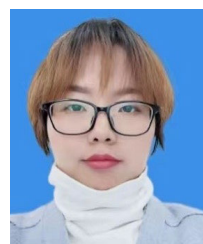
**MENG WANG** received the Graduate degree from Zhengzhou University. He is currently with Jiangsu Huibo Robot Technology Company Ltd. His research interests include industrial robots and artificial intelligence algorithms.

**KHALID A. ALATTAS** (Member, IEEE) received the B.Sc. degree in computer science from King Abdulaziz University, Saudi Arabia, the M.Sc. degree in telecommunication networks from New York University, NY, USA, and the M.Sc. and Ph.D. degrees in computer science from the University of Louisiana at Lafayette, USA. He is currently an Assistant Professor with the College of Computer Science and Engineering, University of Jeddah, Saudi Arabia. His research interests include networks, machine learning, data analytics, robotics, and unmanned vehicles. He serves as a reviewer for many international journals.

**ARDASHIR MOHAMMADZADEH** received the B.Sc. degree from the Sahand University of Technology, Tabriz, Iran, in July 2011, the M.Sc. degree from the K. N. Toosi University of Technology, Tehran, Iran, in September 2013, and the Ph.D. degree from the University of Tabriz, Tabriz, in November 2016. In December 2017, he joined the University of Bonab, Bonab, Iran, as an Assistant Professor. He joined the Shenyang University of Technology as a Professor, in September 2022. His research interests include control theory, fuzzy logic systems, machine learning, neural networks, intelligent control, electric vehicles, power systems control, chaotic systems, and medical systems. He is an academic editor and a reviewer of many journals.

**LILI WU** received the Graduate degree from Hangzhou Dianzi University. She is currently with the Zhejiang Guangsha Vocational and Technical University of Construction. Her research interests include intelligent control, mathematical modeling, and algorithm research.

**HAIYAN HUANG** is currently an Associate Professor with the Zhejiang Guangsha Vocational and Technical University of Construction. Her research interests include intelligent control, mathematical modeling, and algorithm research.

**EBRAHIM GHADERPOUR** received the Ph.D. degree in theoretical and computational science and the Ph.D. degree in remote sensing in Canada, in 2013 and 2018, respectively. He is currently an Assistant Professor with the Department of Earth Sciences, Sapienza University of Rome, Italy. He is also the CEO of Earth and Space Inc., Calgary, Canada. His research interests include big data analytics and artificial intelligence with their applications in remote sensing, geology, geosciences, robotics, and medicine. He is an academic editor and a reviewer of many journals.

● ● ●